Simulating Convection Sensitivity to Atmospheric State During AMIE-Gan

Anthony Del Genio[1]   Audrey Wolf[2]   Jingbo Wu[2]
[1]NASA GISS, New York, NY   [2]Columbia University, New York, NY

Introduction

The relationship between moist convection and tropospheric humidity is thought to be central to the existence of the Madden-Julian Oscillation. The difficulty that many GCMs have in simulating the MJO may therefore be diagnostic of insufficient coupling between convection and humidity in their cumulus parameterizations, associated with weak entrainment and/or rain evaporation. The AMIE-Gan deployment of the second ARM Mobile Facility (AMF2) in the Maldives over the past fall and early winter offers an unprecedented opportunity to observe the onset of the MJO and constrain entrainment in cumulus parameterizations.

MJO Index and MWR PW during AMIE-Gan

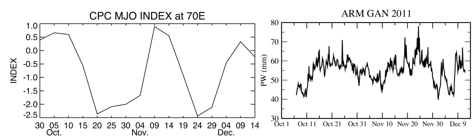

Nature cooperated by producing two strong MJO events during the AMIE-Gan deployment. The figure at the left above shows the NOAA CPC pentad MJO index vs. time during AMIE-Gan. A value of the index < -1 is considered to be indicative of the disturbed phase of an MJO event. MWR measurements of column precipitable water (PW) at Gan during AMIE (above right) vary by 15-20 mm, from values below (~40 mm) to above (~60 mm) the threshold for the transition from weak to strong precipitation (Bretherton et al. 2004; Neelin et el. 2009).

BBSS temperature anomalies and relative humidity during AMIE-Gan

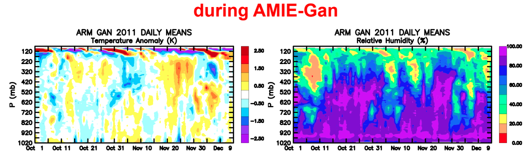

One of the highlights of AMIE-Gan is the presence of a long record of three-hourly radiosonde data. The soundings above clearly show moistening of the lower troposphere by 20-30% relative humidity in advance of MJO onset, followed by 20–30% humidity increases at upper levels after the disturbed phase begins. The temperature signal of the MJO is weaker, but for at least the second observed MJO in November 2011, there is a detectable 0.5-1 K warming of the lower/middle troposphere before MJO onset and ~1.5 K upper troposphere warming after disturbed phase onset.

Wheeler-Kiladis diagrams for GISS GCM control, experiment 1

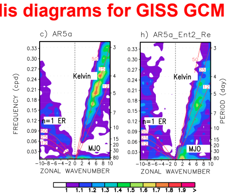

We use the available soundings directly in semi-prognostic SCM simulations that test the response of the parameterizations to the observed thermodynamic structure. We diagnose convection depth using 3 different versions of the GISS Model E2 SCM:

Control: The CMIP5 version with 2 convective plumes (weakly and strongly entraining with $\varepsilon = C B/w^2$, C = 0.3, 0.6) and weak rain evaporation
Experiment 1: Stronger plume 1 entrainment (C = 0.4) and rain evaporation
Experiment 2: Weakly entraining plume exists only after downdraft onset

The Control has no MJO (left panel above), while Experiment 1 (right panel above) and Experiment 2 (not shown) do (Kim et al. 2012).

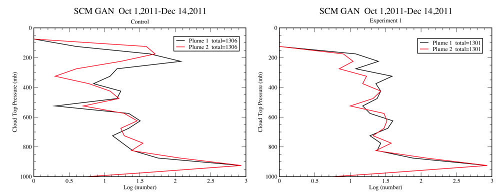

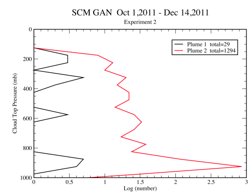

Distribution of convective cloud top heights

When initialized with the Gan soundings, the SCM convects 37% of the time. Most of these are shallow convective events with tops near 925 mb. In the Control run, the distribution is bimodal, with a secondary peak in the upper troposphere and only a small number of instances of midlevel congestus clouds. Plume 2, which nominally entrains more strongly than plume 1, actually penetrates deeper in some cases because of an artificial limiter that resets entrainment to zero when the plume mass exceeds a predetermined threshold. In Experiment 1, this limiter is removed, the entrainment rate of plume 1 is increased (though still weaker than plume 2), and rain evaporation is made stronger as well. As a result, convection penetrates less deeply on average, with more congestus events than in the Control run, and plume 1 produces deep convection somewhat more often than plume 2. In Experiment 2, plume 1 is only allowed to exist when a convective downdraft formed in the previous timestep and penetrates the boundary layer with colder than average air. This crudely mimics the often observed enhancement of deep convection by convergence and lifting at the gust front after cold pools form. For the thermodynamic structure given by the Gan soundings, this occurs very infrequently (< 1% of the time), and so most of the mass flux is carried by plume 2.

Convective tendencies of temperature and specific humidity

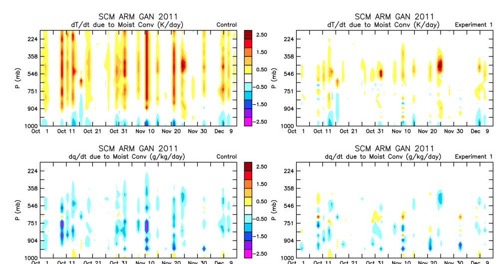

The figures above show the vertical profiles of temperature and specific humidity tendencies vs. time for the Control run and Experiment 1. The Control version consistently produces deep heating and drying throughout the troposphere except in the boundary layer, indicating an absence of moistening by shallow and congestus convection that is essential to the recharge-discharge theory of the onset of the disturbed phase of the MJO. This is consistent with the fact that this model version does not produce MJO-like variability. Experiment 1 produces primarily mid-tropospheric heating, with only occasional significant heating above the 400 mb level. It also produces cooling in the lower troposphere at certain times, consistent with rain evaporation, although net moistening of the lower troposphere occurs only occasionally, near 700 mb. It is not clear whether this behavior is or is not realistic, since even during the suppressed MJO phase, satellite observations indicate a mix of shallow and deep convective events (Del Genio et al. 2012). It may be possible to address this question when the AMIE-Gan large-scale advective forcing product becomes available.

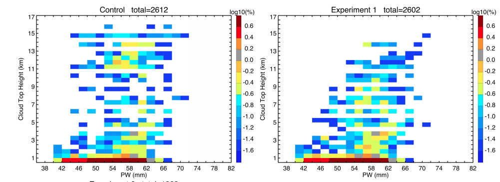

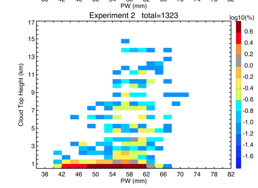

Histograms of cloud top height vs. PW

The Control run shows little sensitivity of convection depth to precipitable water, producing fairly frequent deep convection in even relatively dry (PW < 50 mm) conditions. With stronger entrainment (Experiment 1), convective cloud top heights are shallower overall but especially in drier environments, producing a tendency for convection depth to increase with PW. When weak entrainment is restricted to convective events after cold downdraft onset (Experiment 2), a clear tendency for convection depth to increase sharply with PW emerges, with deep convection only when PW > 54 mm.

Thermodynamic structure for deep and shallow convective events

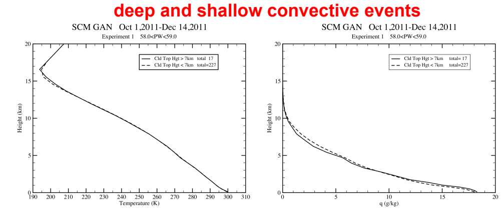

Precipitation studies indicate a large variance in rainfall rate at intermediate values of PW (Neelin et al. 2009). The SCM is consistent with this only in Experiment 1 and Experiment 2, which simulate the full range of convection depths only at intermediate PW. To understand how the cumulus parameterization differentiates between deep and shallow convection at a given PW, we collected two subsets of soundings within the narrow range 58 < PW < 59 mm. One subset contains soundings for which the SCM predicts convective cloud top heights > 7 km ("deep"), the other with soundings for which the predicted convection depth is < 7 km ("shallow"). The figures above show that the temperature profiles are almost identical for both subsets except just below the tropopause. The moisture profiles are systematically different, though: A slightly wetter PBL produces deep convection despite the drier mid-troposphere, while a slightly drier PBL produces shallow convection despite moister than average air above.

Conclusions

✧AMIE-Gan soundings show lower troposphere moistening in advance of the MJO disturbed phase and upper troposphere heating after the onset of the disturbed phase.

✧The CMIP5 GISS SCM, given the observed soundings, makes excessive deep convection; a version with stronger entrainment and rain evaporation reduces convective cloud top height and produces more congestus clouds.

✧The CMIP5 model simulates deep convection independent of the column PW amount. With stronger entrainment there is a gradual transition from shallow to deep convection as PW increases; the transition is sharper when weak entrainment is restricted to events following cold downdrafts.

✧Variance in convection depth for a given intermediate value of PW in the model is determined primarily by fluctuations in boundary layer humidity; a wetter/drier PBL favors deep/shallow convection.